Experimental Investigation of Supercavitating Motion of Bodies

Yu.N. Savchenko
Ukrainian National Academy of Sciences - Institute of Hydromechanics
8/4 Zhelyabov str., 03057 Kiev
Ukraine

1. Modeling the supercavitation processes

1.1. FEATURES OF SUPERCAVITATING FLOWS

Supercavitation naturally occurs when the speed of a subsurface craft increases at fixed pressure P_0. At considerably low speeds (V > 3 m/sec), supercavities form when an object crosses the free water surface. In this case cavities are filled by atmospheric air and refer to artificial cavities formed at low speeds [4, 18].

According to the hydrodynamic scheme of supercavitation flow, the object is placed partially or fully inside a supercavity (Fig. 1a, b) formed by the nose part (cavitator) [1, 4, 6]. In the case of a jet cavitator system the cavity separates from the craft hull (Fig. 1c) and body has no points of contact with cavity [17].

The hydrodynamic drag formulae for continuous and cavitation flow have the form

$$X = C_x(\mathrm{Re})\frac{\rho V^2}{2}S, \qquad X_c = C_c(\sigma)\frac{\rho V^2}{2}S_c \tag{1}$$

and suggest that X_c does not depend on viscosity. Here, $\mathrm{Re} = VL/\nu$ is the Reynolds number; $\sigma = (P - P_c)/(\rho V^2)/2$ is the cavitation number, S and S_c are the characteristics of the wet surface in continuous and cavitation flow, and ρ and ν are the density and viscosity of water.

A qualitative estimation of the respective hydrodynamic drags indicates that with $\sigma = 10^{-4}$ the resistance to motion reduces by a factor of 1/1000.

However, for all its attractiveness due to a low hydrodynamic drag, the motion of an object in a cavity is a more complicated and paradoxical process than that of a space rocket. Moving in a vapor- or gas-filled cavity, the cavitating body loses buoyancy – the main advantage of motion in water, and thus needs dynamic means to maintain its weight inside the cavity [17].

The classical stability condition for motion in a continuum requires that the center of mass of the body should lead the external force application point. In the supercavitation motion scheme, this condition is violated in the most unfavorable way: the hydrodynamic forces are applied in the foremost point of the object – far ahead of the center of mass (Fig. 2). Moving in a cavity with a subsonic speed relative to water (V_a=1430 m/s), the object moves at a supersonic speed V = 4M relative to the vapor filling the cavity as if it were 24 km above the sea level.

Paper presented at the RTO AVT Lecture Series on "Supercavitating Flows", held at the von Kármán Institute (VKI) in Brussels, Belgium, 12-16 February 2001, and published in RTO EN-010.

While, in the continuous flow, the energy expended to overcome the hydrodynamic drag is irreversibly lost in the wake, in the supercavitation flow, the energy of a cavity of length L_c travels with the object of mass m. Their total energy is

$$E_\Sigma = E_0 + E_c = \frac{mV^2}{2} + \int_0^{L_x} X_c \, dl.$$

It is paradoxical that at the moment when the cavity collapses around the body moving in water by inertia with decreasing speed, the velocity suddenly increases. However, this velocity gain occurs in agreement with the energy conservation law. The cavity returns to the body the energy it expended earlier to form the cavity. This effect was found in experiments with cavitating models moving along a wire. In free motion, the imploding cavity can not only disturb motion stability but also destroy the body.

It should be noted that the problem of cavity closure, including hulls of vehicless, is a large field of research with applications to generation of supercavities and reduction of dynamic drag to levels below X_c.

In view of these specific features of supercavitation flows one may conclude that the feasibility of this motion scheme is contingent on the stability of object motion in the cavity. Therefore, in experimental launches in water, spherical bodies have been used more frequently than others [9]. In some flows, cavity embraced only a part of the hull, while the aft remained wet to preserve the stability of motion (see Fig. 1a).

In experimental investigation we realize a processes of physical modeling the supercavitation flows which includes three separate but associate problems:

1) modeling the supercavity shape and dimensions;
2) modeling the main SC processes as gas supply, gas leakage, SC creation, SC control, SC disturbanse;
3) modeling the supercavitating body motion.

We consider sequentially these problems from point of view of the theory of dimensionality and similarity of the hydrodynamic flows. Application of methods of the theory of dimensionality and similarity permits:

– to determine the minimal number of dimensionless parameters describing main sides of the studied process;

– to choose a rational scheme of the laboratory experiment;

– to obtain rules of recalculation of the experimental results for full-sc

ale magnitudes of the parameters.

Foundations of the theory of dimensionality and similarity and this theory application to different fields of the hydromechanics are stated in books

[1, 2].

1.2. MAIN SCALES AND PARAMETERS GOVERNING THE SUPERCAVITATION PROCESSES

For stationary supercavitation flows the process is defined by the following parameters [29]:

– characteristic linear size of the body L;

– pressure difference in the free stream and cavity

$p_\infty - p_c$;

– fluid velocity V_∞;

– fluid density ρ;

– gravity acceleration g;

– kinematic coefficient of the water viscosity υ;

– coefficient of water surface tension ζ.

There are three basic measurement units: length, time and mass. According to Π - theorem of the theory of dimensionality [1], it is possible to give no more than 7 – 3 = 4 independent dimensionless combinations of enumerated parameters. The other flow parameters and acting forces are functions of such four scaling parameters.

The cavitation number σ, the *Froude* number *Fr*, the *Reynolds* number *Re* and the *Weber* number *We* are used as main scaling parameters:

$$\sigma = \frac{2(p_\infty - p_c)}{\rho V_\infty^2}, \qquad Fr = \frac{V_\infty}{\sqrt{gL}}, \qquad \mathrm{Re} = \frac{V_\infty L}{\nu}, \qquad We = \frac{\rho V_\infty^2 L}{\zeta}. \tag{2}$$

Cavitator diameter D_n is usually used as linear scale L for supercavitation flows.

Equality of four scaling parameter guarantee observance of geometric, kinematic and dynamic similarity of stationary supercavitating flows. Namely, the cavity section diameters D and acting forces F may be calculated by formulae:

$$D\left(\frac{x}{D_n}\right) = D_n f_1(\sigma, Fr, \mathrm{Re}, We), \qquad F = \frac{\rho V_\infty}{2} D_n^2 f_2(\sigma, Fr, \mathrm{Re}, We), \tag{3}$$

where f_1, f_2 are dimensionless functions of dimensionless parameters. They can be once and for all determined theoretically and experimentally..

Moreover, only equality of cavitation drag coefficients c_X of the cavitators, but not the geometric similarity of them is necessary for the supercavitating flows. The cavitators with the same diameters D_n and drag coefficients c_X forms cavities of approximately equal sizes. When values of σ are low and values of *Fr* are high, mid-section diameter D_c and length L_c of the axisymmetric cavity past a disk are approximately equal [2, 3]:

$$D_c = D_n \sqrt{\frac{c_x}{\kappa\sigma}}, \qquad L_c = D_n \frac{A\sqrt{c_x}}{\sigma}, \qquad A = \sqrt{\ln\frac{1}{\sigma}}, \tag{4}$$

where κ = 0.9 ÷ 1.0 is the empirical constants. It is shown in [2, 4] that formulae (4) may be used and for non-disk cavitators of different shape, if the universal linear dimension $D_n\sqrt{c_x}$ is accepted as characteristic linear dimension instead D_n.

When values of σ are small, the approximate relation is valid for the drag coefficient of blunted cavitators [2, 3]:

$$c_x(\sigma) = c_{x0}(1+\sigma), \qquad 0 < \sigma < 1.2, \tag{5}$$

where c_{x0} is the cavitator drag coefficient at $\sigma = 0$. For disk cavitator it is established that $c_{x0} = 0.82$.

However, simultaneous equality of numbers σ, Fr, Re, We is impossible to reach in practice. Therefore, investigation of scaling effects, i.e. influences of different deviation from similarity is of great importance in modeling the supercavitation processes.

1.3. SUPERCAVITIES IN STEADY FLOWS: MODELING BY THE σ NUMBER

The cavitation number σ is main scaling criterion of the supercavitation flows. The value of $\sigma <$ 0.1 corresponds to the supercavitation regime. Such values of the cavitation number are reached at velocities V_∞ > 50 m/s. It is established experimentally [2, 3] that the water viscosity influence is practically absent at such velocities in the case of the disk cavitator and free cavity closure. Influence of gravity and surface tension forces also are negligible when

$$Fr > 20 \div 30, \qquad We > 1000. \tag{6}$$

Thus, for natural supercavities the functions f_1, f_2 in (3) depend on only dimensionless parameter σ being unique scaling criterion of the flow.

We obtain the empirical formula for the natural supercavity shape [5]:

$$\overline{R}^2(\overline{x}) = 3.659 + 0.847(\overline{x} - 2.0) - 0.236\sigma(\overline{x} - 2.0)^2, \qquad \overline{x} \geq 2.0 \tag{7}$$

where $\overline{R} = R / R_n$, $\overline{x} = x / R_n$. In this case we used an analysis of the experimental data obtained for the models with D_n = 15 mm and the range of cavitation numbers σ = 0.012 ÷ 0.057. The frontal cavity part $\overline{x}$ < 2.0 is described by the empirical formula [3]

$$\overline{R} = \left(1 + \frac{3x}{R_n}\right)^{1/3}, \qquad \overline{x} < 3 \div 5, \tag{8}$$

The following expressions for the cavity mid-section and length are obtained from the formula (7):

$$\overline{R}_c = \sqrt{3.659 + \frac{0.761}{\sigma}}, \tag{9}$$

$$\overline{L}_c = 4.0 + \frac{3.595}{\sigma}. \tag{10}$$

Expressions (9), (10) are in good agreement with results of our experimental investigations of high-speed motion of small supercavitating models in water [5] (D_n = 1.0 ÷ 3.0 mm). The cavitation numbers $\sigma = 10^{-4} \div 10^{-3}$ and Mach numbers $M = V_\infty / a = 0.3 \div 0.9$ (where a = 1460 m/s is the sound speed in water) correspond to these experiments. Thus, the water compressibility influence on the main cavity dimensions may be considered as nonessential one at motion velocities up to 1200 m/s.

A practical advantage of formula (7) is that it gives the explicit dependence of the cavity shape on the cavitation number.

1.4. ARTIFICIAL SUPERCAVITIES IN STEADY FLOWS: MODELING BY THE *Fr* NUMBER

It follows from the theory of similarity of hydrodynamic flows that the shape and dimensions of natural and artificial (ventilated) cavities must be equal at the same value of σ . However, this is not observed in reality.

The main cause is that the moderate values of the *Froude* number $Fr < 20$ correspond to the flows with artificial cavitation when motion velocity V = 10 ÷ 50 m/s. It means that the gravity importance for artificial cavity is essentially greater at equality of the cavitation numbers.

As it is known , gravity forces influence on the artificial cavity by double ways.

Firstly, the cavity axis is curved (the cavity floating-up), and the cross section shapes calculable by the perturbation method [6] are deformed.

It is known from the experiments, and theoretical investigations confirm that the liquid crest forms below the cavity when the cross gravity field acts. Its top increases in direction from the cavitator to the cavity tail. Sometimes, this crest is small even in the cavity end, and the cavity does not transform into two vortex tubes. In other cases the crest top already past the mid-section may reach the upper cavity part and cleave it on two tubes.

In the work [6] important criterion was obtained by theoretical way:

$$N = \sigma \sqrt{\sigma} Fr^2 \geq 1.5. \qquad (11)$$

It is possible to emphasize the following ranges of changing the parameter N. They corresponds to different conditions of perturbations caused by fluid gravity:

1) range N = 1 ÷ 2 is characterized by high perturbation levels, when all cavity part after the mid-section degenerates in vortex tubes;
2) range N = 2 ÷ 4 corresponds to mean or essential perturbation level, when the water crest height is lower than the unperturbed cavity radius, although may be close to it;
3) range N = 4 ÷ 10 is characterized by low perturbation level, and gravity influence may be egligible when

$N > 10$.

In Fig. 3, a, b, the calculation results of shape of cross cavity sections when cavitation numbers σ = 0.06 and *Froude* numbers Fr = 10 are shown. In this case N = 1.47. In sections 1, 2, 3, when x = 0.25 and x = 0.50, the gravity action yet does not appear, and in section, when x = 0.75, small compression

from below is already appreciable. In sections 4, 5, when x = 1.25, the deformation is considerable. It is close to half of the radius value below the section. The crest directed up is well seen. In the next sections the cavity collapses.

Secondly, the cavity closure behavior and type of gas leakage from the cavity change. It was established experimentally [2, 3], that the influence of viscosity and surface tension is not essential. Thus, in this case the flow is determined by two scaling criteria σ and Fr.

However, it is difficult practically to obtain simultaneous equality of numbers σ and Fr . Modeling by the cavitation number requires simultaneous decrease of the model dimension to save the *Froude* number value. A way of the gravity force compensation in rotating hydro-tunnels is known [2].

A method of physical modeling of the gravity influence on the supercavity shape by means of curving the external flow was proposed in the work [7]. The flow was curved in the vertical plane due to bend of the working part bottom (Fig. 4). For such flow the numbers Fr depends on bottom curvature radius R_b:

$$Fr = \frac{V}{\sqrt{\left(g - \frac{V^2}{R_b}\right) D_n}}. \tag{12}$$

To change fluently the *Froude* number in range $20 < Fr < \infty$ was succeeded by curving the flow in the experiments with artificial cavity past a disk when D_n = 20 mm and free stream velocity V = 9 m/s. In this case the characteristic deformation of the cavity owing to the floating-up was completely eliminated. The cross force arising on the cavitator may be easily compensated by corresponding inclination of the cavitator.

The stream curving method is convenient to use for compensation or, on the contrary, intensification of the gravity force action on the artificial cavity shape in hydrotunnels with horizontal flow. It has advantage compared to a method of the rotating hydro-channel [2], since permits to work with models of large longitudinal dimensions. However, we notice that this method does not model the influence of number Fr on the internal processes in the cavity, such as reentrant jet formation and motion of foam and sprays within the cavity.

In the case of unsteady flow the *Strouhal* number is the additional determining scaling parameter:

$$St = \frac{L}{Vt}. \tag{13}$$

The essential difference between natural (vapor) and ventilated supercavities becomes apparent at unsteady flow. Investigations showed that the parameter characterizing the gas elasticity influence in the cavity is of important in this case.

2. Special equipment for experimental investigation

All installations for experimental investigations may be divided on two parts:

I. Installations of inverse motion:

- water tunnels;
- water flumes;
- rotating channels.

II. Installations of direct motion:

- towing channels;
- test basins;
- launching tanks.

The models with full fixation (without levels of freedom) are mainly used under inverted motion.

The models with partial fixation or models with free motion may be used in direct motion. There are wire riding models and models used as missiles.

The inverted motion is limited by velocity range 3 ÷50 m/s so that the high speed motion of SC models must be investigated at direct motion only [17, 18].

2.1. WATER TUNNELS

Experience of development of experimental high-speed hydrodynamics shows that it is convenient for velocities up to 30 m /s to use the inverted motion, which is realized due to water tunnels [16], water flumes and rotating water channels [2, 9].

There are the closed circuit water tunnels as LCC in Memphis and Garfield Thomas Water Tunnel in Pennsylvania.

The Large Cavitation Channel (LCC) of the David Taylor Model Basin, CDNSWC, is a large variable pressure water tunnel and it is one of the most technologically advanced large cavitation tunnels in the world.

IHM has two unclosed circuit water tunnels.

The small WT has a working section is 0.34×0.34 m, the working part length is 2m, the mainstream velocity is 9 m/s. It is a tunnel of open type with opened working part. Pumps inject water to the upper tank, where free level is sustained constant. The water arrives under constant pressure of water column equal to 4.5 m to the working part.

The big WT (Fig. 5) has a working section 1 – $4 \times 0.5 \times 0.5$ m with maximal admissible velocity up to 30 m/s. The supplying part – 2 of the WT has length 35 m is used as a launching tank. It has 10 pairs of looking windows.

The WT has a gas separator – 3. The water arrives in basin – 4 having volume – 4400 m^3 through the separator for the further degassing and comes to the pumps – 5 with total power 5 000 KWt. The photo Fig. 6 demonstrates WT view from separator.

In experimental supercavitation it is very significant to organize supercavity without extra disturbances in rear part of supercavity. A special device (Fig. 7), which can do this, was elaborated at the IHM.

Supercavity generator (Fig. 7) contains struts – 1, cylindrical section – 2, ring type cavitator – 3 with leading edge to produce free boundary – 4 of supercavity – 5.

To decrease disturbances of supercavity this device contains a special pipe line – 7 for boundary layer suction through the ring gap – 6.

The photo below demonstrate the working supercavity generator in the test section of WT.

It should point that the supercavity is very sensitive to changing of surrounding flow in the working part of WT. This change of the flow is caused by the supercavity and called by Blocking effect and may be estimated experimentally.

Fig. 8 shows change of the supercavity under influence of Blocking effect. General recomendations relating to the maximal cross section of the supercavity S_c has the form

$$\frac{S_c}{S_w} \le 0.01,$$

where S_w is the working part section.

2.2. EXPERIMENTAL EQUIPMENT FOR SELF-PROPELLED WIRE RIDING MODEL TESTING

Considerable experience of the creation of such laboratory equipment and carrying out with the help of it the experiments to study the supercavitating flow around models with caliber 40 – 60 mm, when they free move in water at velocities higher than 100 m/s has been accumulated at the IHM UNAS [28]. Application of different power systems of the models is possible in the experiments. The ecologically pure components: water in various phase states and compressed air are used as working medium in them. The body ride system along a guide wire proved to be the most effective to divide the problems of the cavity dynamics and the motion stability by stabilizing the model trajectory in water.

It is possible to note the following advantages of the described technique of the model testing:

– a possibility of studying the supercavitating flow around models of comparatively large caliber at absence of external perturbations;

– enough wide range of the flow velocities and regimes: from artificial ventilated cavitation to natural vapor cavitation in the velocity range V ≈ 50 – 150 m/s;

– possibility of studying of both stable flow regimes and unsteady processes on initial stages of the cavity, development and also adjustment of regimes of water entry of models;

– comparatively large caliber of the tested models gives considerable variety both in the model constructions and in the hydrodynamic schemes of flow around them;

– system of the model trajectory stabilization by means of the guide wire allows the minimal necessary deepening of the trajectory and, hence, simplifies photo-registration of flow pictures through the free surface;

– when optimal conditions of the water entry of the models are ensured, the stabilization of the supercavitating flow regime is reached on very short distance (about some model length) and requires very limited engine power of the models;

– compact laboratory reservoirs of different types: channels, flumes, basins, tunnels etc. may be used to carry out tests due to short working part of the trajectory and effective system of the ydrodynamic braking of models;

– absence of chemical energy sources and use of the water and compressed air in the model power systems as the working medium at moderate high values of the pressure ensure a possibility of safe exploitation of the experimental equipment in laboratory conditions.

Imperfection of the described technique of the testing is mainly complexity of registration of the process characteristics at the model motion in water with high speeds. In this case the basic information is ensured by studying of the model motion kinematics and photo-cinematography of its flow pictures.

Synchronization of work of the registering apparatuses with certain phases of the model motion in water may have certain technical complexity.

Configuration of the model testing system

Here, we interpret the optimal configuration as such set of the system elements and their composition which ensure a possibility of obtaining of the stable motion regimes in a supercavity for different constructive modifications of the models at rational technical parameters of whole system: general dimensions, material capacity and sizes of equipment, energy consumption etc, including the ecological compatibility and exploitation safety. As it was noticed, the type of reservoir used to create the testing system has no principal significance. The following description is based on materials of tests carried out in the hydrodynamic laboratory at the IHM in opened hydroflume with dimensions 1.0 x 1.0 x 40 m. The model motion trajectory was located on the depth 0.5 m along the flume axis. Photo-cinematography of the flow pictures was realized through the glass windows in walls of the flume and through the free water surface.

One of necessary conditions of the supercavity formation on starting stage of the motion in water is enough high velocity of the model which is ensured by means of the starting catapult, i.e. predominantly owing to "cannon effect". In this case the model mass executes a role of the kinetic energy accumulator being able to ensure the stable motion on inertia. In the given case equipping the model by jet engine has no principal significance for its dynamics. The considered here types of the working medium of the engine at their bounded board reserve are able to ensure only very short-term thrust. It does not give decisive difference of the velocity value and is reached by means of the model mass decrease during motion. In some cases, for example, increase of the inertial mass of the model due to filling the hull by material with higher density, for instance, metal may be the more advantageous to increase the free model passage distance at the same starting velocity instead of the engine with working medium reserve. Therefore, in this case use of models with jet engine is of interest for combined study of hydrodynamic aspects of interaction between the cavity and working engine.

Model with water-vapor jet engine

The water-vapor jet engine represents a kind of propulsive device where the direct transformation of the thermal energy into the thrust work occurs, and, simultaneously, hydrodynamic and thermodynamic processes including the phase changes of the working medium proceed.

Hot water application as the working medium of the jets has considerable history. In various time beginning from antiquity different variants of the devices using the reactive vapor jet to carry out the work appeared. Serious works on application of the hot water for missiles began to be carried out, apparently, before the Second World War in Germany and after the War in West Germany, USA, Italy [19 – 22]. An interest to such type of propulsions is stipulated first of all by their economical parameters and ecological factors.

The considerable volume of investigations on thermal hydrojets including water-vapor jet was carried out at the IHM UNAS [23, 24, 25]. The investigations were being performed as applied to a problem on creation of high-speed underwater vehicles using the outboard water for jet work.

The constructive scheme of the model with water-vapor jet is shown in Fig. 9, a. As a whole the model represents a body of revolution with cone nose and cylindrical parts. The cylindrical part 1 of the model hull is made from stainless steel and contains the working medium reserve for the water-vapor jet. The jet nozzle 2 is installed on the hull end and has a central body with tail 3 protruding from the model hull. The tail is intended for joining with the catapult lock and holding the model during the process of heating and water pressure increasing in the model and catapult. The nose cone part 4 of the model hull is isolated hermetically from the cylindrical part 1 and may be made from aluminum for the model mass

decrease. The changeable cavitator 5 is installed on the cone nose 4. The general view of such model with hull diameter 58 mm is shown in photo of Fig. 9, b.

As it is pointed above, tests of the described models were carried out in the flume with dimensions 1.0 x 1.0 x 42 m. The general scheme of the model testing system is presented in Fig. 10. In the scheme numerals designate: 1 is the flume, 2 is the starting chamber produced in the flume by divider 3. In the scheme the starting chamber is shown filled by water. Respectively, the catapult 4 and the model 5 installed in it are located in underwater position. Cameras 6 and impulse illuminants 7 with divergent screen for uniform light background creation are used to register the picture of flow around the model at its motion in the flume. Disposition of the photo-registration means is shown in the scheme in two positions. The position for recording photo-registration means is shown in the scheme in two positions. The position for recording through the glass windows in the flume walls stipulates disposition of the camera and illuminant on the opposite sides of the flume. The position for recording through the free water surface requires the camera disposition above the flume and underwater disposition of the illuminant.

Conditions of carrying out the experiments differed from the calculation ones by final value of the heated water reserve, which was close to the calculated second rate, and inevitable pressure dropping in the chamber of the jet in moment of the model start from the catapult. However, it is possible to suppose that the pointed differences do not essentially influence the jet thrust value for short term of its work. It is less than 0.2 sec at average model velocity 110 m/s and length of the working part of the trajectory about 20 m. This supposition is confirmed by results of tests where the model motion regimes with practically constant velocity along the distance were registered, and photographs of flow around the model were obtained. In these cases the model moved in the supercavity without washing the hull, i.e. its total drag was equal to the nose cavitator drag and corresponded to the thrust developed by the jet. The maximal parameters of heated water was $P = 150 kgf / cm^2$, $t = 320^\circ C$.

Drag value R_x of the disk cavitator with diameter D_n is determined by formula [3]

$$R_x = c_x F_n \frac{\rho V^2}{2}, \tag{14}$$

where $c_x = 0.82$ is the drag coefficient for a disk; $F_n = \frac{\pi D_n^2}{4}$ is the wetted area of the cavitator; ρ is the water density; $V \approx 110$ m/sec is the model velocity characteristic for considered regimes. For models with disk cavitators at $D_n = 12 \div 16$ mm we obtain the cavitation drag magnitudes in the range $R_x = 57 \div 101$ kgf. This satisfactorily corresponds to pointed above calculated value of the jet thrust $T = 87.5$ kgf.

Mentioned above photographs of supercavitating flow around the model without washing the hull are shown in Fig. 11. The presented photographs are made from the different positions: through the free water surface at model velocity $V = 124$ m/s (Fig. 11, a) and through the glass windows in the flume sides at model velocity $V = 106$ m/s (Fig. 11, b). The photographs shows that in the both cases the model jet works in natural vapor cavity, i.e. in the medium with the saturated vapor pressure corresponding to the value accepted in the calculated example value $P_c = 0.02$ kgf/cm^2.

Auxiliary devices of starting chamber

It was pointed above that the developed cavity formation on starting part of the model trajectory in water is a necessary condition of establishing the supercavitating flow regime on the next part of the trajectory. Experience of tests of cavitating self-propelled models showed that the high starting model velocity not always ensures enough fast axisymmetric cavity formation past the cavitator at the underwater start. This mainly relates to the models with small cavitator diameter compared to the hull

diameter. In this connection different types of auxiliary devices intended to regulate conditions of water entry of model and optimize the cavity formation past the cavitator were tested in the IHM. Such devices were mounted in the start chamber of the flume with the catapult installed in it. It is shown in scheme Fig. 10. Description of some types of pointed auxiliary devices is given below.

One of ways of optimization of the cavity formation process consists in organization of water entry of the model through the initial air bubble. A scheme of such bubble creation for underwater start conditions is presented in Fig. 12. The catapult 1 with installed in it model 2 is shown in the scheme. The ring distributive chamber 3 with ring nozzle 4 is installed coaxial to the model near the cavitator. The compressed air is supplied by the main 5 to the device. The air supply is regulated by the electric valve 6. In the start moment the air bubble 7 may be obtained by choosing the ring chamber and nozzle parameters, the compressed air pressure and moment of its charging into the water. This air bubble maintains orientation along the model axis for short term. In this case the air from the bubble may be entrapped into the cavity and promote its formation process. However, the test showed that the described device does not guarantee stable results. Possible explanation of this consists in non-uniformity of the internal bubble structure with chaotic distribution of the water and air masses.

The most stable results by ensuring the cavity formation were obtained at model start from the dry start chamber according to the scheme given in Fig. 13. In this case in the partition 1 separating the flume 2 filled with water from the dry start chamber the hatch 4 is closed by movable gate opening the hatch 4 just before the start. As a result, the contrary water jet 5 is formed, and the model enters in it after the start from the catapult. Favorable conditions for the supercavity formation past the cavitator are stipulated by two factors: atmospheric air entrapment and that the pressure in free flowing jet is equal to the entrapped atmospheric air.

However, uncontrolled entrapment of the atmospheric air into the cavity is undesirable in a number of cases. Such situation takes place, for example, at studying the quantitative characteristics of the air supply influence on the cavity formation process. In such cases the water entry of the model may be organized according to the scheme presented in Fig. 14. For that the entrance hatch 2 is covered by elastic plastic diaphragm 3 in the partition 1 separating the dry start chamber from the flume filled by water. At start the model 4 punches the diaphragm serving as an elastic seal hindering the atmospheric air penetration into the zone filled by water. In this case the initial cavity 5 forms under influence of a established beforehand value of the supply realized from the model.

Model attachment mechanism

The local features of flow around the cavitator at the model motion along the wire are illustrated by photographs and scheme in Fig. 15, a,b. The presented illustration shows that the zone in front of the cavitator, where the fixed wire is located, must be excluded from the consideration when the quantitative characteristics are determined. Therefore, so called effective value D_{ef} of the cavitator diameter is accepted for calculations. Its area is equal to the wetted area of the real cavitator [2, 3] by formulae

$$D_{ef} = \sqrt{D_n^2 - d_w^2}\,.$$

Such approach validity is illustrated by experimental results of the cavity profile measurements at different conditions of flow around the cavitator. They are given in Fig. 16. The experimental data in the graph are compared with the cavity profile equation proposed by *G.V.Logvinovich* [3]:

$$\frac{D}{D_c} = \sqrt{1 - \left(1 - \frac{D_1^2}{D_c^2}\right)\left(1 - \frac{2x}{L_c}\right)^2}\,,$$

where D, x are current diameter and coordinate of the cavity section; D_c, L_c are the cavity mid-section diameter and length, respectively; $D_1 = 1.92 D_n$.

Model arresting mechanism

It is necessary to ensure fluent arresting the model up to its stoppage at the model trajectory end. A simple and effective mechanism in the form of installed with some intervals metal disks with diameters scaling up is the most convenient for this purpose. The testing system scheme shown in Fig. 10. gives a general presentation about such mechanism. There are shown the arresting disks 9 in the end part of the flume 1 filled by water on the wire 8. They are coaxial with it. The model in turns meets them on its path. Orifices in the disk centers permit them to be free removed along the wire. In rest water the disks are in given position. After contact with the model they move together with it as cavitators with sequentially increasing diameters and hydrodynamic drag value. During arresting the model pushes on a set of such disks in front of it up to complete stoppage.

The scheme in Fig. 17 shows this process the more in detail. Obviously, the cavity dimensions decreases, the hull washing area increases, and on the end part of the arresting path the model moves in unseparated flow regime as a result of the motion velocity reduction. Correspondingly, three typical parts of the arresting path are shown in the scheme. The regime of flow around the model is qualitatively changes on these parts. There are: part I with predominantly cavitation flow regime, part III with unseparated flow regime and part II between them with transient regime. Thus, hydrodynamic side of the model arresting process is enough complex.

It is important from practical point of view that the described mechanism permits to give by the simplest means any required intensity of the arresting from very fluent reduction of the model velocity to abrupt its stoppage. The necessary effect is reached by choosing the arresting disk diameters and intervals between them The arresting process intensity may be regulated in very wide limits by changing one of the pointed parameters.

2.3. EXPERIMENTS WITH FREELY MOVING MODELS

Vertical vacuum launching tank (VVLT)

VVLT (Fig. 18) consists of cylindrical tank, that is installed under different angles to horizon. There are a catapult, windows and device to capture models on the tank (arresting system). The VVLT contains the system of pressure control and system of underwater launch.

The VVLT gives the possibilities for wide range experiments with freely moving models. It is possible to change an angle between the model velocity and horizon and between the model velocity and the model axis and to investigate the model motion under different trajectory inclination and different model incidence.

The problems of body water entry at supercavitation regime, the ricochet problem, body motion stability on underwater trajectory were investigated successfully by using the VVLT.

The Fig. 18 shows the frames of high speed photo registration of supercavitating body motion at water entry under angle to the free surface of water.

The Fig. 19 shows the instant pictures of water entry investigation with supercavity inception control by using the metal or rubber rings on the body hull. During water entry the rubber ring produces a local pressure field suppressing the supercavity inception.

35 m Launching Tank

At the IHM the supplying part of Big Water Tunnel is used as a 35 m Launching Tank with the cross section is 2.2 ×2.2 m (Fig. 20). This tank has 10 pairs of glass windows and may be supplied by an pneumatic or electrochemical catapult using electrolysis gas energy by electric decomposition of water [30].

$$H_2O \Rightarrow 2H_2 + O_2 \Rightarrow 2H_2O + 152 kcal.$$

The Fig. 21 shows the scheme of experiments in the launching tank. The launching tank – 1 contains 10 pair of windows – 2. The catapult – 3 may be used in two positions for underwater launch:

Position 1 – out side of tank. The catapult is connected with launching tank only by end of barrel through the hole – 4.

Position 2 – inside of tank. The catapult is placed completely in the water tank.

A steel shield – 6 is used as arresting system for supercavitating models – 5. It is in another end of the launching tank.

Photo-registering system has cameras and sparkle lamps working through the glass windows – 2 (Fig. 20).

The Fig. 22 demonstrates the view of launching tank with catapult in position –1 (out side of water tank).

The Fig. 23 shows the supercavitating model cartridge. There are supercavitating model – 1, container – 2 assembled with two parts with help rubber ring – 3 and piston – 4.

The Fig. 24 demonstrates the frames of high speed photo-registration of supercavity produced by moving projectile having a cone shape and disk cavitator – 3 mm with velocity 1000 m/s when $\sigma = 10^4$. The supercavity length and diameter were 12 m and 0.11 m, respectively.

References

1 Sedov L.I.. Methods of similarity and dimensionality in mechanics. 7th Edition. - Moscow, Nauka, 1972. 428 p., (in Russian).

2 Epshtein L.A. Methods of theory of dimensionality and similarity in problems of ship hydromechanics. – Leningrad: Sudostroenie, 1970. 208 p., (in Russian).

3 Logvinovich G.V. Hydrodynamics of flows with free boundaries. - Kiev, Naukova dumka, 1969. 208 p., (in Russian) .

4. Epshtein L.A. Characteristics of ventilated cavities and some scale effects. // High-speed unsteady water flows (Proc. of international simp. IUTAM) – Moscow, Nauka, 1973. P. 173-185, (in Russian).

5 Savchenko Yu.N., Vlasenko Yu.D., Semenenko V.N. Experimental study of high-speed cavitation flows. //J. Hydromechanics. 1998, # 72. P. 103-111, (in Russian).

6 Buyvol V.N. Slender cavities in flows with perturbations. - Kiev: Naukova dumka, 1980. – 296 p., (in Russian).

7 Savchenko Yu.N. Developed cavitation modeling in flume with curved flow. // J. Hydromechanics. 1974. – # 26. P. 3-5, (in Russian) .

8 Epshtein L.A., Lapin V.M. Approximate calculation of influence of flow boundaries on cavity length in two dimensional problem and past the axisymmetric body. // Trudy TsAGI - 1980. # 2060. P. 3-24, (in Russian).

9 Knapp R.T., Daily I.W. Hammitt F.G. Cavitation. McGraw-Hill Book Co., 1970.

10 Savchenko Yu.N., Semenenko V.N., Osipenko S.B. Mechanism of interaction between cavity and bubble flow. // Reports of AS of Ukraine. 1985. N 9. P. 39 – 42, (in Russian).

11 Savchenko Y.N., Semenenko V.N. The gas absorption into supercavity from liquid–gas bubble mixture. //Proc. Third International Symp. on Cavitation. Vol.2. Grenoble (France). 1998. P. 49-53.

12 Savchenko Yu.N., Semenenko V.N., Putilin S.I. Unsteady processes during supercavitating body motion. // J.Applied Hydromechanics. 1999, Vol. 1, N 1. P.62-80, (in Russian).

13 Semenenko V.N. Computer simulation of supercavitating body dynamics. //J. Applied Hydromechanics. –2000, Vol. 2, N 1. P. 64-69, (in Russian).

14 Pernik A.D. Problems of cavitation. –Leningrad: Sudostroenie, 1966. 335 p. (in Russian) .

15 Levkovsky Yu.L. Structure of cavitating flows. Leningrad: Sudostroenie, 1978. 222 p., (in Russian).

16 Gorshkov A.S., Rusetsky A.A. Cavitation tunnels. – Leningrad, Sudostroenie, 1972.

17 Savchenko Yu.N. On motion in water at supercavitation flow regimes. // J. Hydromechanics, # 70. Kiev: Naukova dumka. 1996. P. 105 – 115.

18 Kirschner Ivan N. Supercavitating projectile experiments at supersonic speeds. High Speed Body Motion in Water. AGARD Report 827. Published February 1998.

19 Kolle H.H. Uber die Wirtschaftlichkeit von Wasserdampfraketen als Horizontal –Starthilfen. – Munchen, 1955.

20 Schwarzler K., Untersudiungen an Hiess Wasserraketen zum Start von Flugzeugen. – Zeitschrift fur Flugwissenschaften 6. Tahrgang, Heft 1. Januar, 1958.

21 Etheimer I.P. Beitrage zu den Problemen der Heisswassseraketen. – Luftfahrt. Forschungsber. 1962, # 12.

22 Tunge Tohn F. Steam rocket successfully tested. Missiles and Rockets. 1962. 11.

23 Babitsky A.F., Ivchenko V.M. Jet theory of thermal hydrojet.// J. Hydromechanics, # 5. Kiev: Naukova dumka. 1968. P. 67 – 78.

24 Logvinovich G.V. Work of jet with ejector nozzle. // J. Hydromechanics, #19. Kiev: Naukova dumka. 1971. P. 3 – 9.

25 Ivchenko V.M., Prihodko N.A., Grigoriev V.A. Optimal jet systems. Krasnoyarsk. Krasnoyarsk University Publishing House. 1985. 218 p.

26 Utkin G.A. Formulation of problems on dynamics of elastic systems with objects moving along them. // Wave dynamics of machines. – Moscow: Nauka, 1991. P. 4 – 14.

27 Kazhayev V.V., Utkin G.A. Motion of mass along wire under action of wave pressure forces. // Differential and integral equations. Gorkiy: Publ. House of GSU, 1989. P. 112 – 117.

28 Vlasenko Yu.D. Supercavitating roket model experiments// Applied Hydromechanics. V. 2, #3. 2000. P. 26 – 39.

29 Savchenko Yu.N. Modeling of supercavitation processes// Applied Hydromechanics. V. 2, #3. 2000. P. 75 – 86.

30 Savchenko Yu. N. Investigation of High-Speed Supercavitating Underwater Motion of Bodies. AGARD Report 827 "High Speed Body Motion in Water", 1998, FDP Wokrshop, Kiev. – P. 20-1 – 20-12.

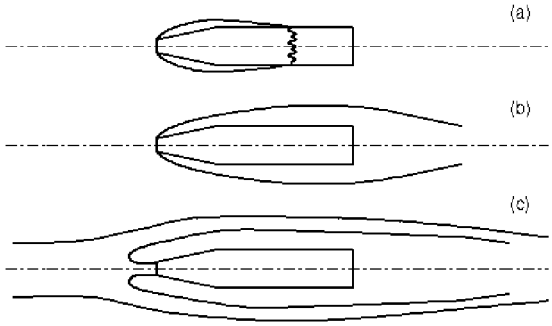

Fig. 1

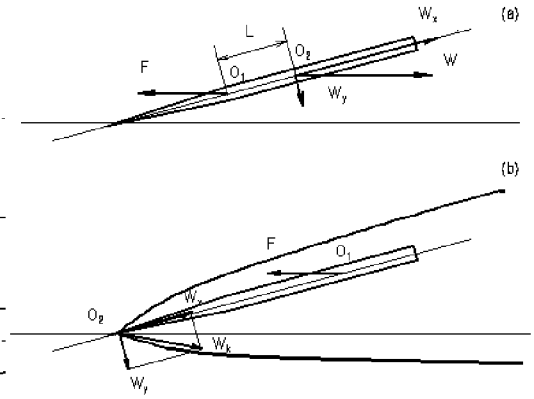

Fig. 2

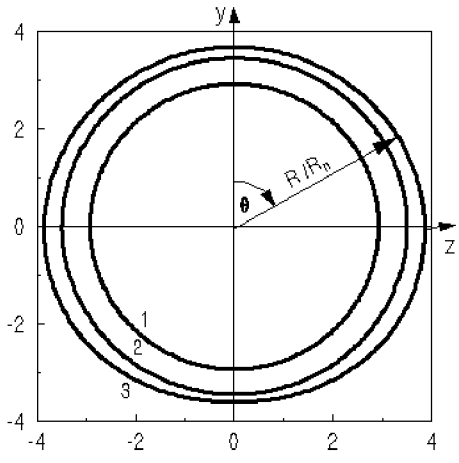

Fig. 3a

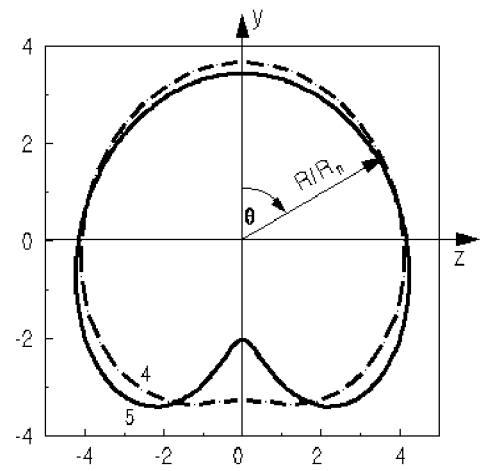

Fig. 3b

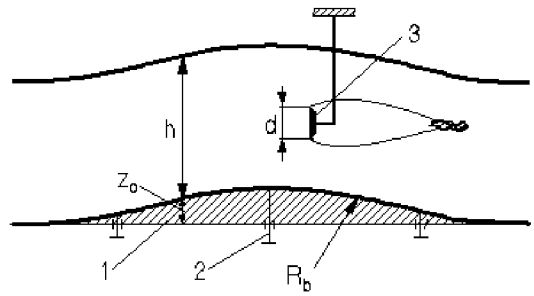

Fig. 4

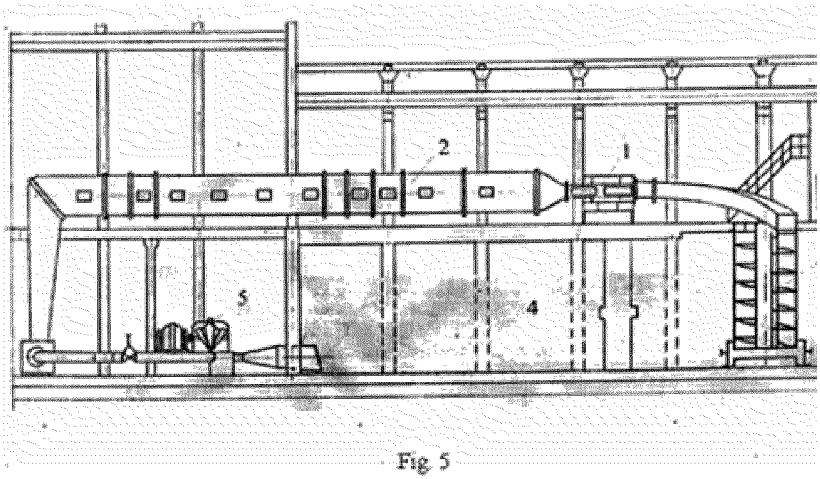

Fig. 5

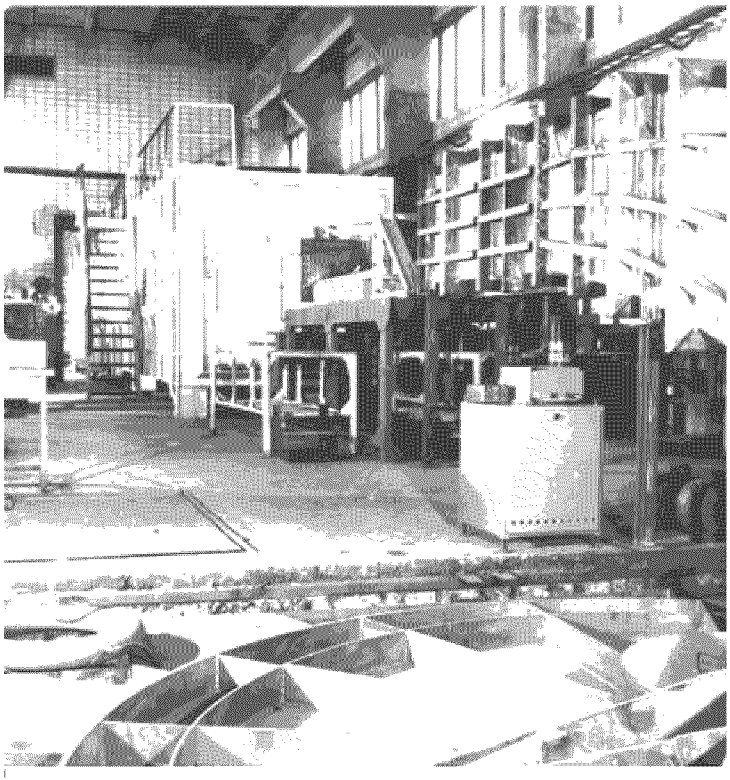

Fig. 6

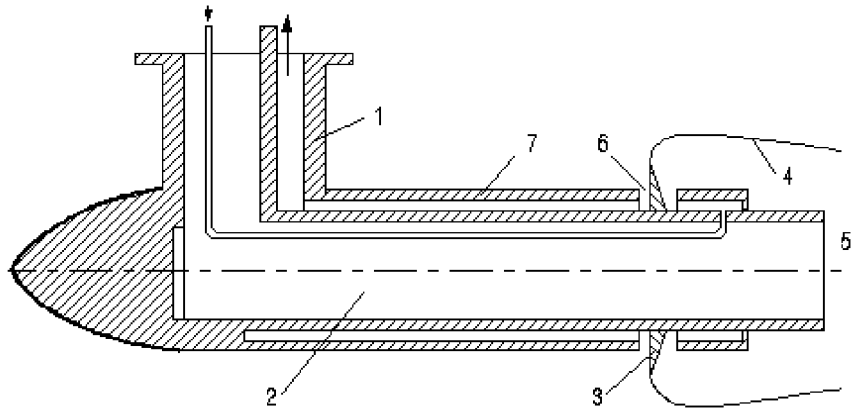
1
7
6
4
5
2
3

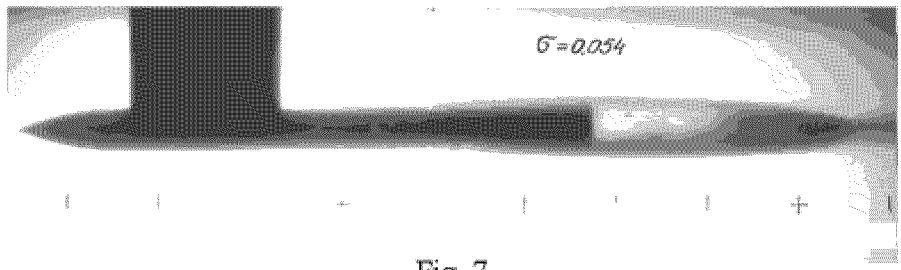
σ=0.054

Fig. 7

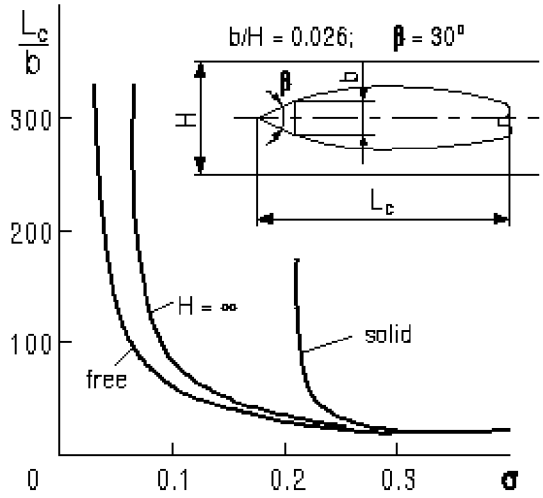
Lc/b
b/H = 0.026;
β = 30°
β
b
H
Lc
300
200
100
0
0.1
0.2
0.3
σ
H = ∞
solid
free

Fig. 8

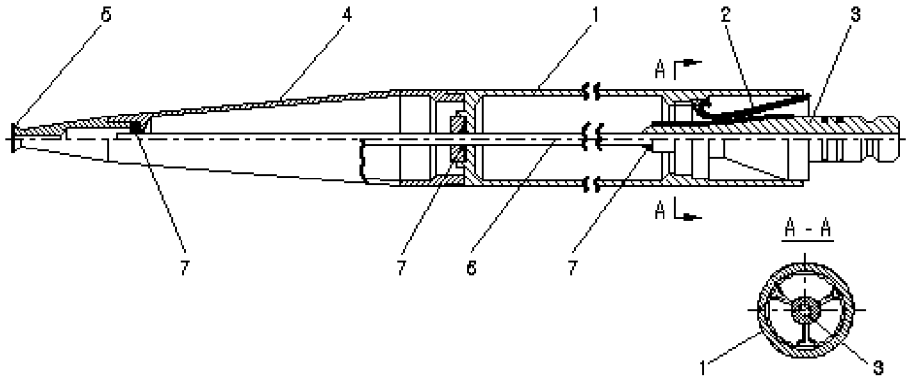

Fig. 9a

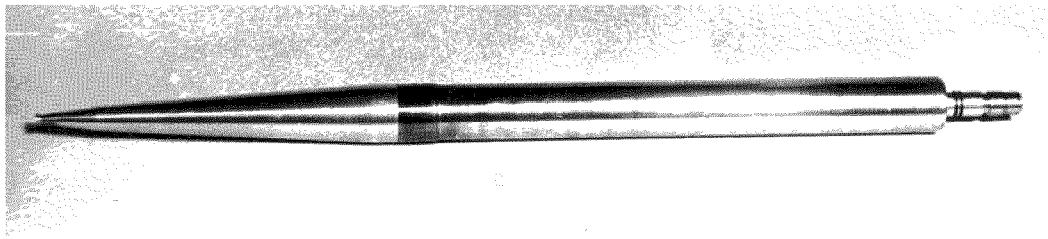

Fig. 9b

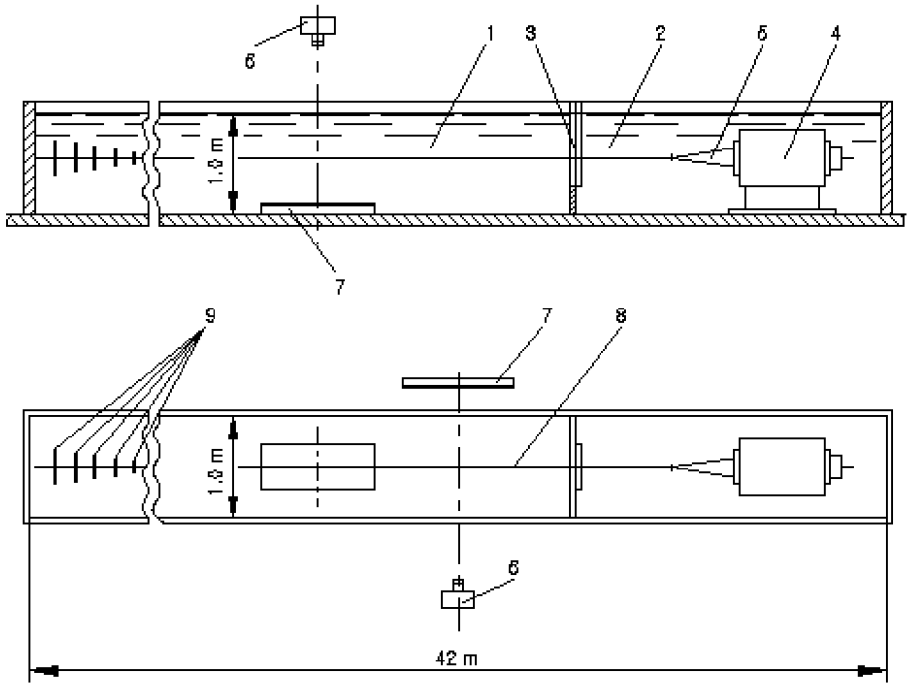

Fig. 10

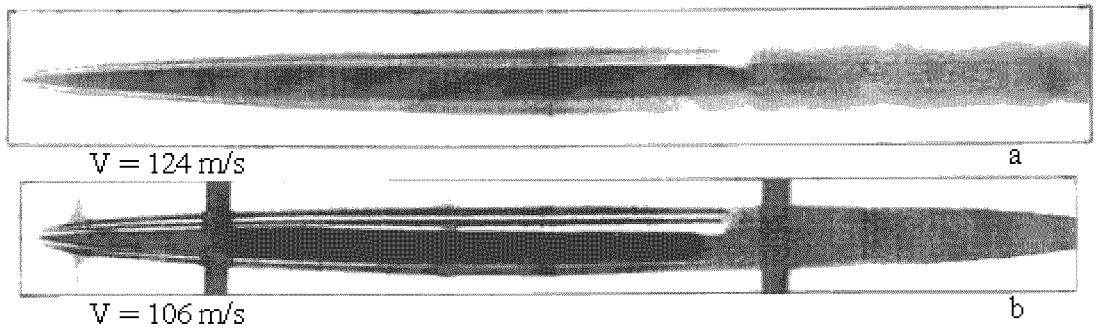

Fig. 11

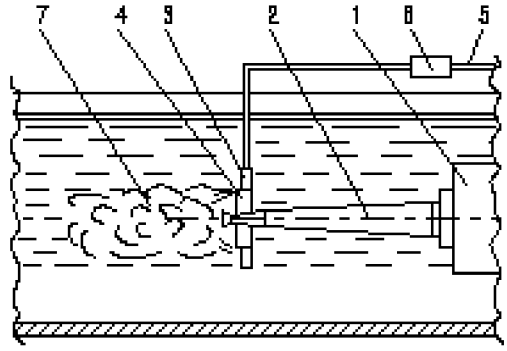

Fig. 12

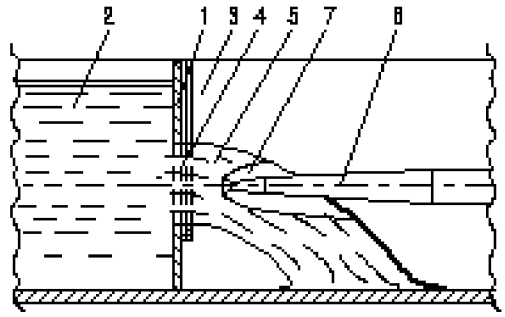

Fig. 13

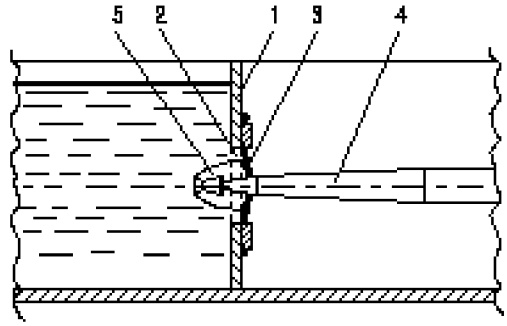

Fig. 14

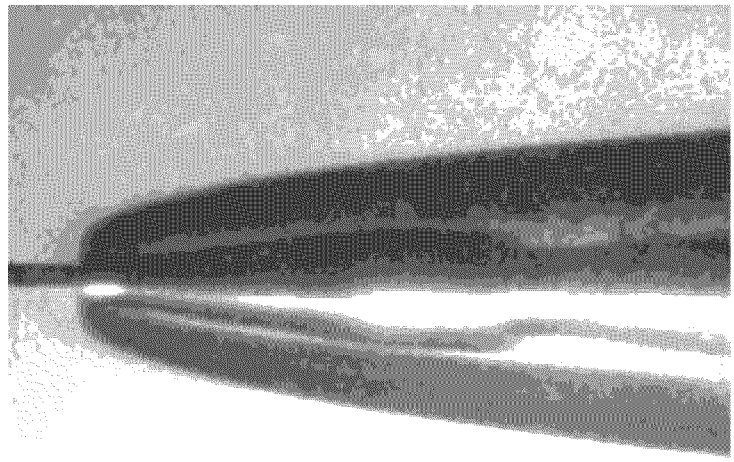

Fig. 15a

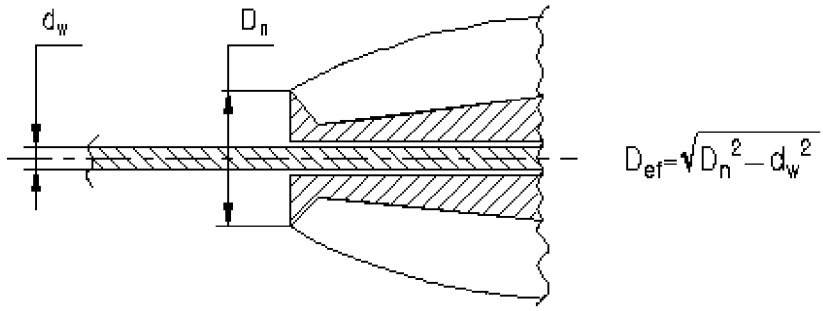

Fig. 15b

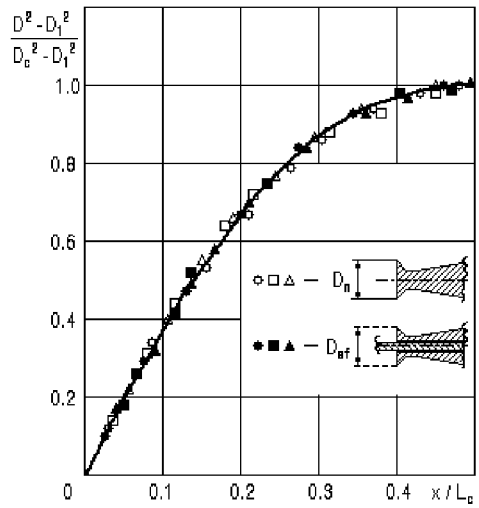

Fig. 16

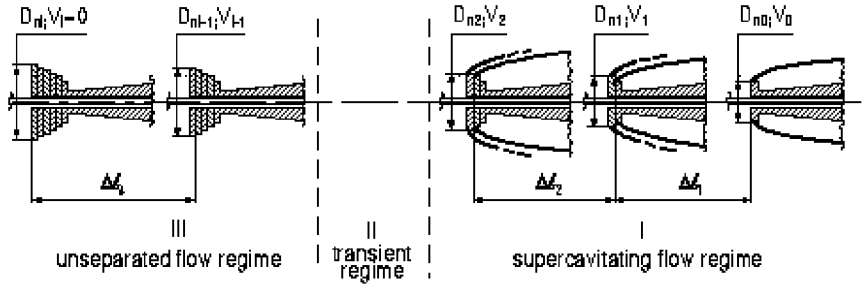
$D_{n};V_{l}=0$
$D_{n1-1};V_{1-1}$
$D_{n2};V_2$
$D_{n1};V_1$
$D_{n0};V_0$
ΔL_3
ΔL_2
ΔL_1
III
unseparated flow regime
II
transient regime
I
supercavitating flow regime

Fig. 17

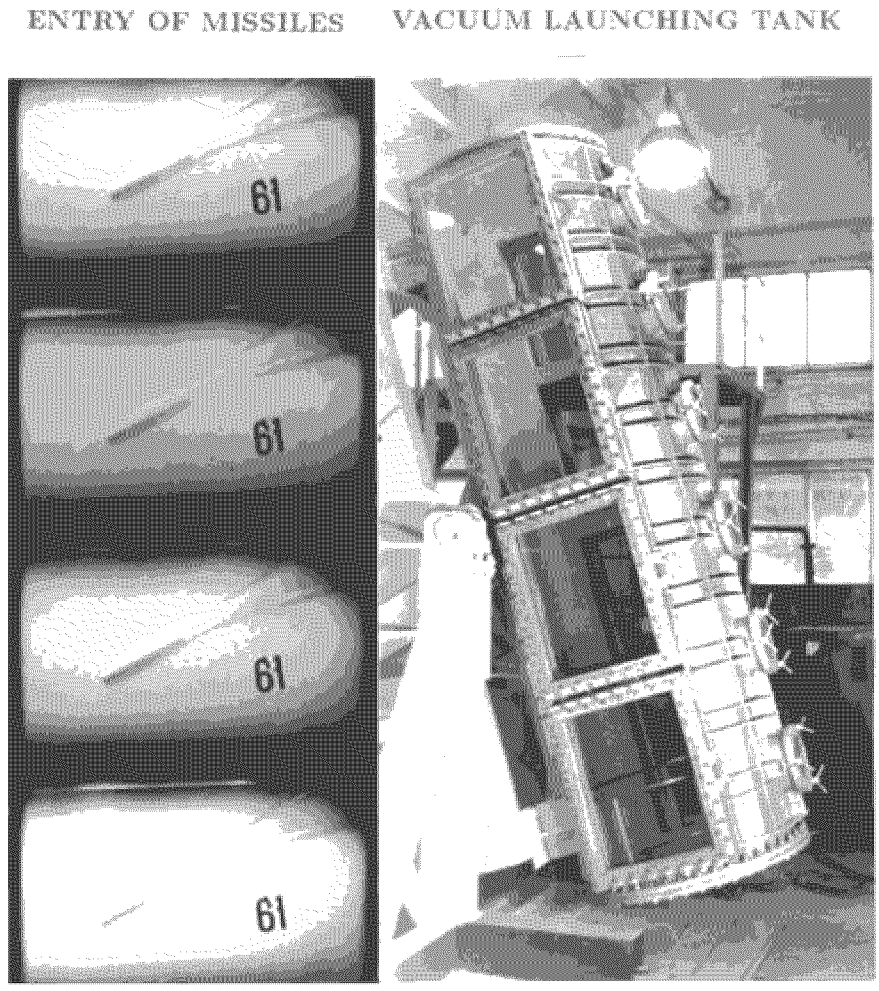
ENTRY OF MISSILES
VACUUM LAUNCHING TANK
61
61
61
61

Fig. 18

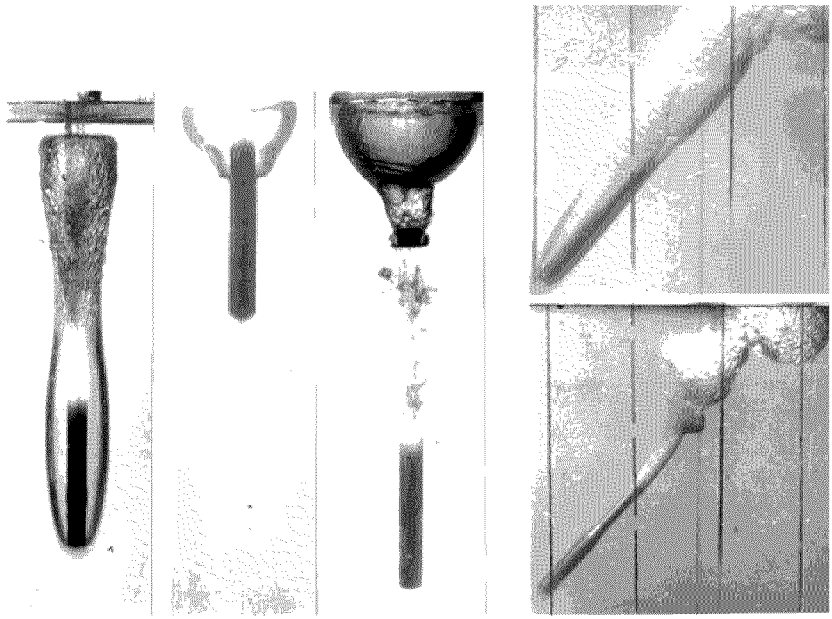

Fig. 19

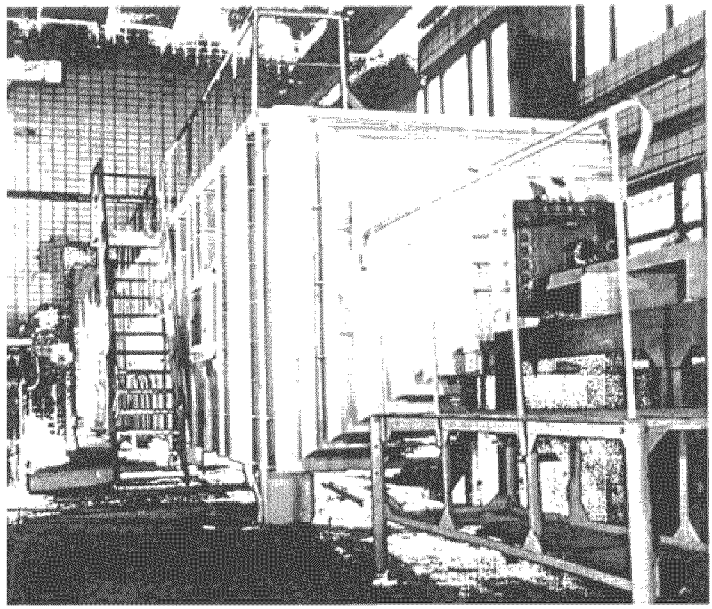

Fig. 20

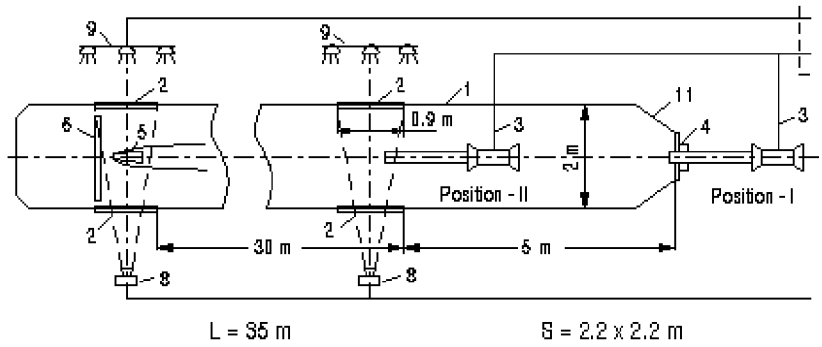

Fig. 21

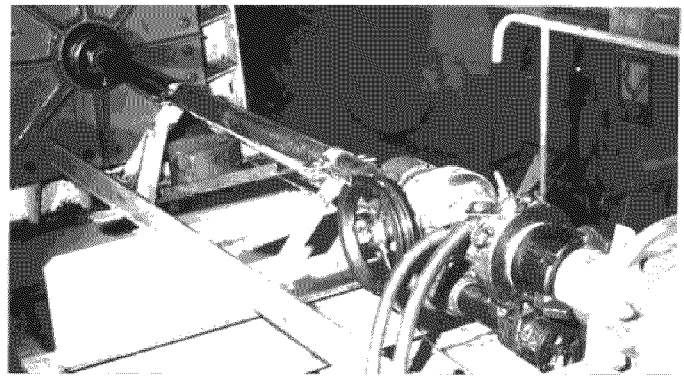

Fig. 22

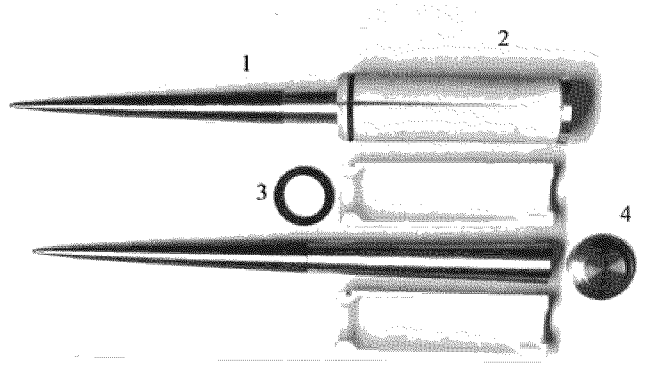

Fig. 23

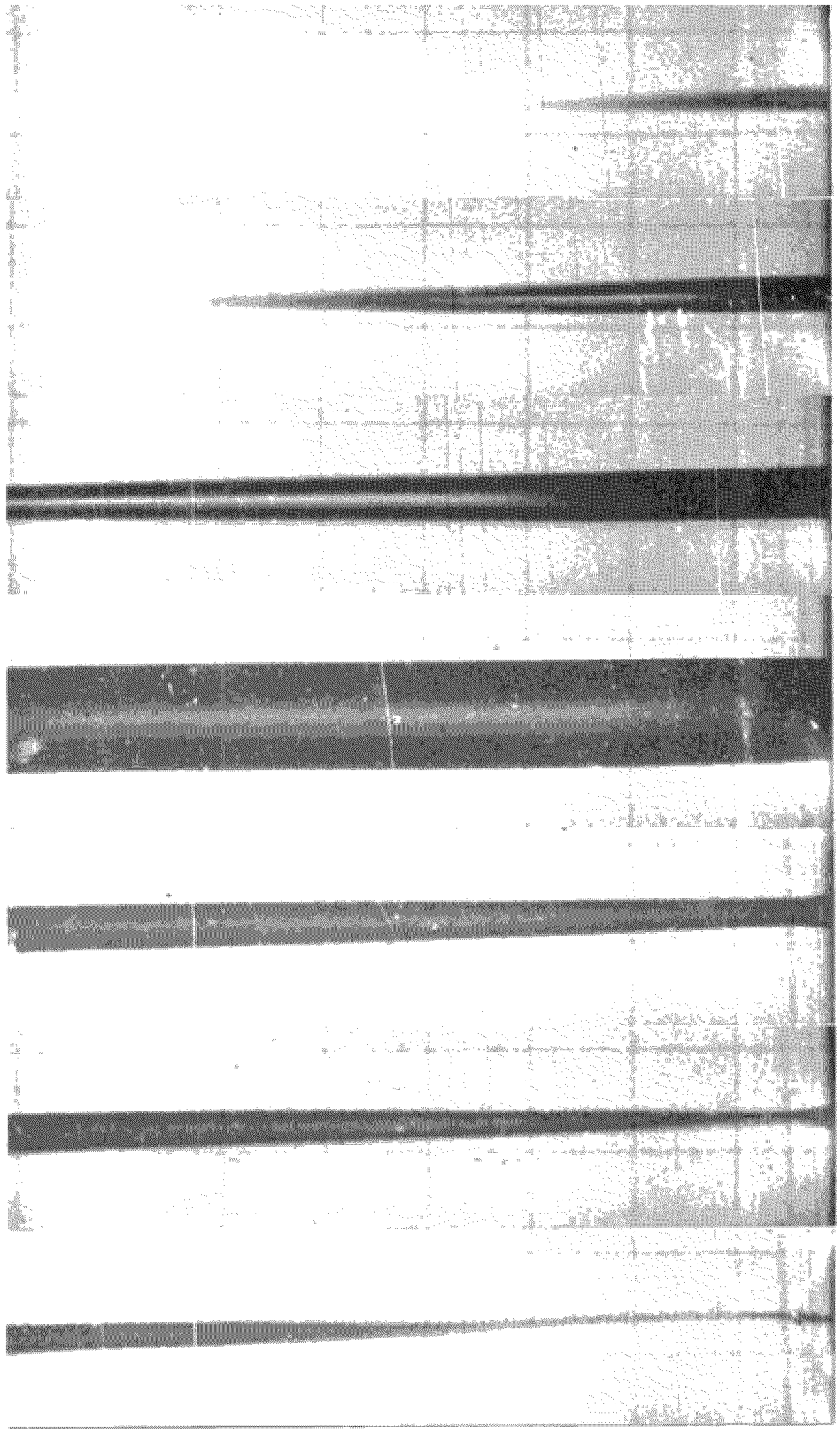

Fig. 24